On land mobile satellite navigation performance degraded by multipath reception

Andreas Lehner, Alexander Steingaß
Institute of Communications and Navigation, German Aerospace Center (DLR)

BIOGRAPHY

Andreas Lehner was born in Gmunden, Austria in 1973. He received his diploma engineer degree in Mechatronics from the University of Linz in 2001. Since then he has worked as a research scientist at the German Aerospace center DLR, focusing on measuring and modelling of multipath propagation, interference measurements, studies on satellite navigation performance for land mobile, indoor and aeronautical applications, and on rail collision avoidance systems.
Homepage: http://www.dlr.de/kn/kn-s/lehner
Email: andreas.lehner@dlr.de

Alexander Steingaß was born in Mettmann, Germany in 1969. He received his Dipl. Ing. diploma in Electrical Engineering in 1997 (University of Ulm, Germany). Since then he has been a research scientist at the German Aerospace Centre DLR – Institute of Communications and Navigation. He has been involved in several projects in the area of satellite navigation and location dependent mobile services. In 2002 he was promoted Dr. Ing. at the University of Essen.
Homepage: http://www.dlr.de/kn/kn-s/steingass
Email: alexander.steingass@dlr.de

ABSTRACT

In this paper simulation results of DLR's ultra-wideband land mobile satellite (LMS) multipath channel model are presented. The goal is the evaluation of GNSS performance in the rail environment. For this safety of life (SOL) application an urban railway was identified as the most critical scenario. The channel model is based on a measurement campaign of the land mobile multipath channel performed in 2002. From this data a model was derived that is synthesising the measured channel impulse response. It allows the realistic simulation of the multipath channel by approximating every single reflection. This model includes time variant reflectors approaching and receding in dependency of the azimuth and elevation of the satellite. All the signal processing had been realised independently of the transmitted signal. Therefore the usability for both, navigation systems GPS as well as GALILEO is given.

1. INTRODUCTION

Besides the ionosphere one of the most significant problems to achieve an accurate navigation solution in cities with GPS or GALILEO is the multipath reception. Various channel models do exist for ground to ground communications (e.g. COST 207 for the GSM system). But there was a lack of knowledge for broadband satellite to earth channels [1]. Therefore the German Aerospace Centre (DLR) performed a measurement campaign in 2002. In this campaign we used a Zeppelin to simulate a satellite transmitting a 100 MHz broadband signal towards earth. To ensure a realistic scenario the signal was transmitted between 1460 and 1560 MHz just nearby the GPS L1 band. This signal was received by a measurement van and was recorded using a regular time grid. The so gathered data was then passed through a super resolution algorithm to detect the single reflections. In a further step we tracked the detected reflections in time and gained knowledge about the characteristics of any isolated reflection. This includes both Doppler shift and delay of the reflection. On top of this we gained knowledge about the direct path behaviour.

2. DIRECT PATH

In an open environment the direct path would be best represented by the line of sight (LOS) transmission of the signal. In an urban environment this LOS signal is often blocked so that the first received path is attenuated and possibly delayed with respect to the LOS. In cities we had been able to identify three major types of obstacles that influence the signal reception.

1. House fronts
2. Trees
3. Lampposts

2.1 The influence of house fronts

When the LOS ray is going to be blocked by a house front the signal is obviously affected. **Figure 1** shows the vehicle on a track during the measurement driving into the shadow of a building. The x-axis indicates the driven distance from start. At about 3886 m the vehicle is entering the shadowed area. From this instance on the signal is strongly attenuated. This behaviour is well known from the so called ”Knife Edge Model” [2]. In this model it is assumed that a planar wave is hitting a half sided infinitively large plate. The calculated attenuation from this model is also displayed in Figure 1. From this comparison the similarity of measurement and model is obvious. Therefore the knife edge model is selected to model this effect. This process is motion dependent only.

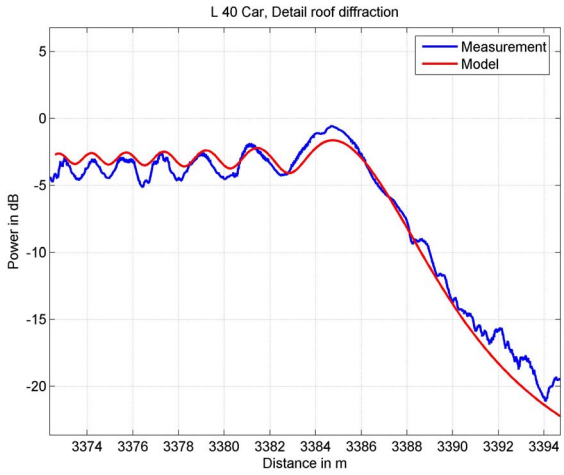

Figure 1: Diffraction by a house front measurement in comparison to the model used

2.2 The influence of trees

As it is shown in **Figure 2** the LOS signal can be attenuated by trees. The measured process on the one hand side is dependent on the length of the LOS signal being within the tree, on the other hand side an additional process is visible caused by branches and leafs. In contrast to approaches where branches and leafs are modelled as very complex scatterers [3] we use a combination of an attenuating only cylinder modelling the transmission through the tree and a statistical fading process modelling the branches and leafs. This process is motion dependent only.

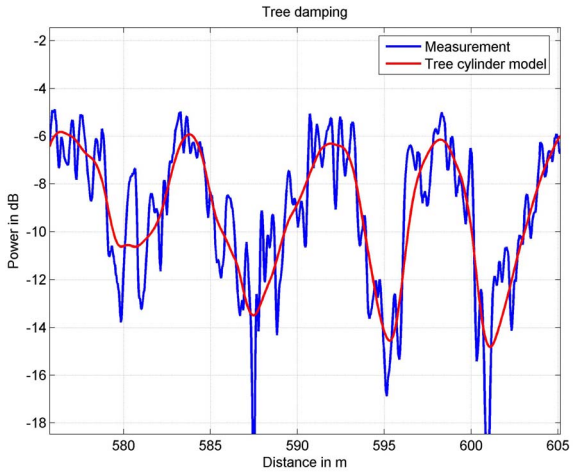

Figure 2: Signal attenuation by series of trees - comparison of measurement and cylinder model

2.3 The influence of lampposts

Surprisingly a lamppost has a strong effect on the LOS signal. **Figure 3** shows an example of a lamppost with a diameter D of 20 cm. When passing by such a post the strength of the signal begins to oscillate, goes down quickly in the direct shadow of the post and comes up again oscillating behind. We model a lamppost with a ”double knife edge model” where we assume two overlapping knife edge plates being present. One is reaching from $-D/2<x<\infty$ and the other is reaching from $-\infty<x<D/2$. Both edges are simulated separately and then added coherently. **Figure 3** shows the near perfect match of model and measurement. This process is also motion dependent only.

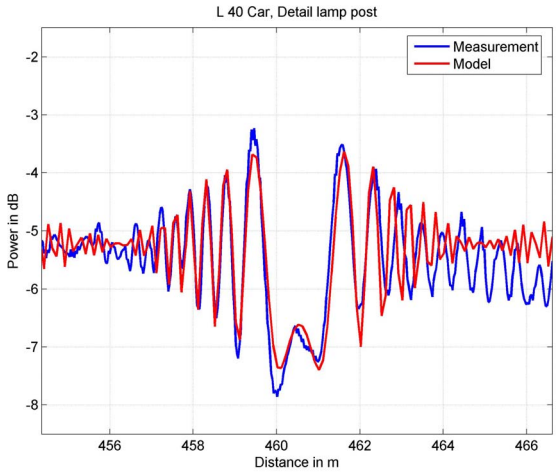

Figure 3: LOS signal being affected by a lamppost - comparison of measurement and model

3. THE REFLECTED SIGNAL

In the measurement data many reflections appear in the urban environment [4, 5]. In contrast to ray tracing algorithms [6] we do not model a specific scenery. We assume reflections to be statistically distributed in the x,y,z space and generate them statistically. In order to match the measured statistic we must take a closer look at the echo distribution.

3.1 Influence of the relative azimuth angle

Let us assume a receiver to be at position RX, a satellite at position S and a reflector at position R. Then the relative azimuth receiving angle α is the angle at the receiver (see **Figure 4**). We can see a clear dependency on the relative azimuth angle in the measurement data (**Figure 5**) with a maximum of the likelihood distribution at α= 180°. For this figure we averaged over all occurring absolute azimuth angles θ by

$$\overline{p}(\alpha) = \frac{\sum_{\theta_i} \frac{p(\alpha|\theta_i)}{p(\theta_i)}}{\sum_{\alpha_i}\sum_{\theta_i} \frac{p(\alpha_i|\theta_i)}{p(\theta_i)}} \quad . \tag{1}$$

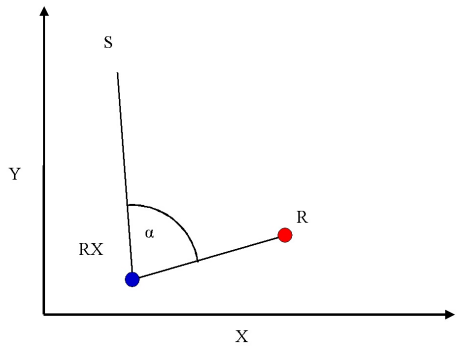

Figure 4: Definition of the angle α.

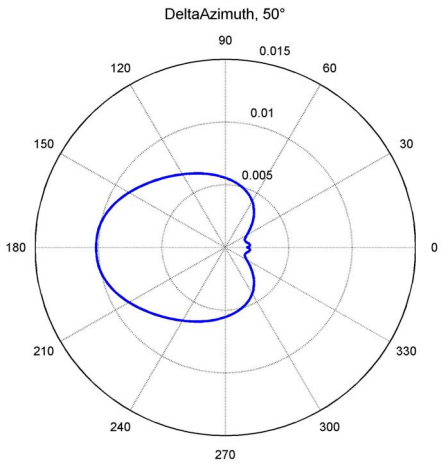

Figure 5: Likelihood distribution of the relative azimuth angle α (at 50° elevation).

This on the first look astonishing result can be easily understand if one has in mind the very rectangular structure of urban cities. Due to this structure a corner reflector (see **Figure 6**) occurs very often in cities. The main characteristic of this reflector is that a ray coming from a satellite is being reflected back into the satellite direction in the x-y plane. Its elevation is unchanged. Then it is obvious that it is most likely to receive reflections from the opposite side of the satellite.

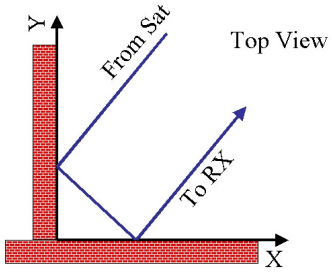

Figure 6: Corner reflector as it can be often found in cities.

3.2 Geometric occurrence of reflectors

Figure 7 shows the likelihood distribution of reflectors in a top view. In this figure the receiver is moving in x-direction only. It can clearly be seen that the highest likelihood of receiving a reflector is when the reflector is on the right or on the left side. The likelihood of receiving a reflector from the front is close to zero. This as well on the first look astonishing result becomes more plausible when one has an urban canyon in mind. It must be unlikely that a reflecting obstacle is in near front position of the car, otherwise one would overrun it in the next second. To calculate the conditional likelihood of a reflector being present at a certain position for a specific satellite azimuth one has to multiply the statistics shown in **Figure 5** and **Figure 7**. The result of this operation is shown in **Figure 8**, here the satellite position had been chosen at 25° azimuth.

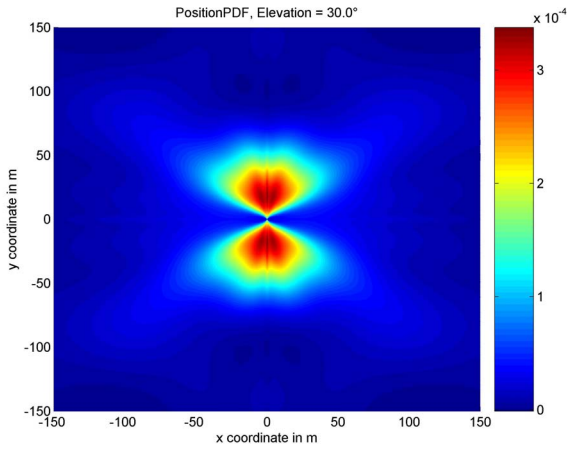

Figure 7: Likelihood of reflectors being at a certain 2-D position (receiver movement in x-direction only).

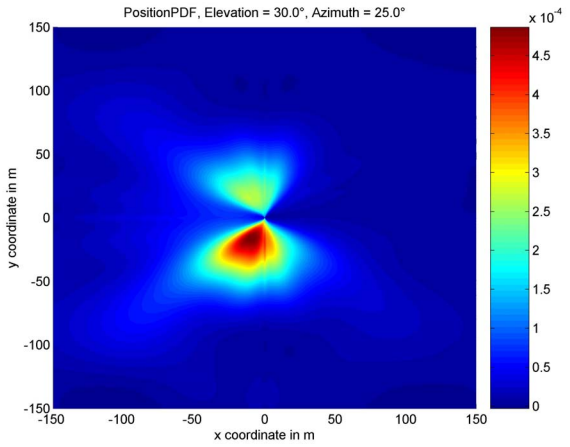

Figure 8: Conditional likelihood of reflectors being at a certain 2-D position. Satellite at 25° azimuth

3.3 Lifespan of reflectors

In the measurement data the channel appears rapidly changing. Many echoes disappear and others appear at new positions. This process is highly correlated to the receiver speed. When the car stops the reflections remain in the

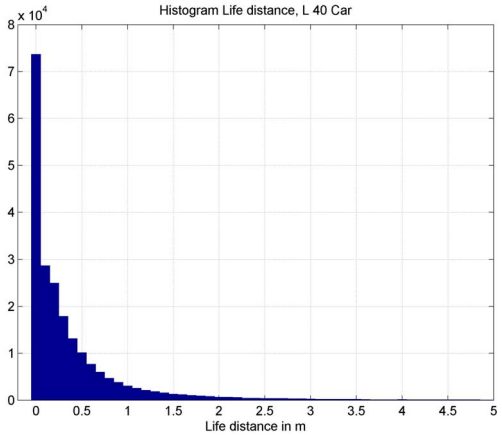

Figure 9: Live distance of echoes

scenery. Therefore we defined a life distance of each reflector. This life distance is the distance the receiver is travelling until the echo disappears. **Figure 9** shows a histogram of the echo life distances. It can be seen that the life distance of the reflectors is usually well below 1 m. Most reflectors exist along a motion path below 5 m. Therefore the channel is changing rapidly.

3.4 Mean power of reflectors

Figure 10 shows the power distribution in dependency of the relative position. Since reflectors in the real world have a given geometrical size of course their distance plays a major role for the mean

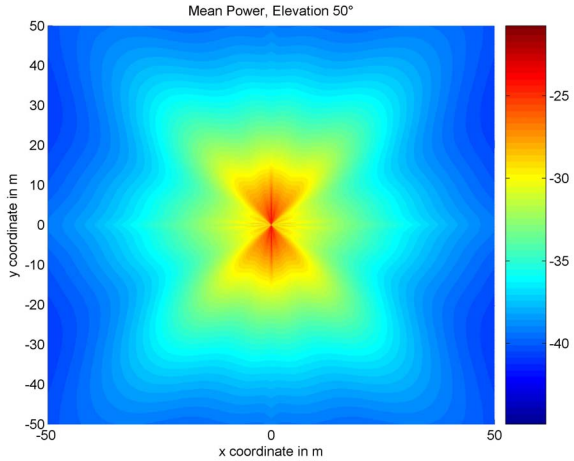

Figure 10: Mean power of the reflectors in dependency of their relative position.

received power. Having again in mind the urban canyon, it is quite understandable that the most powerful reflections are on the sides of the streets. With increasing distance the mean power of the reflections is decreasing. Beside the mean power map we have derived a power variance map (not shown) to allow a certain variation in this process, like we observed it in the measurements.

3.5 Fading process of reflections

When a car drives through an urban environment, the receiver moves through a quasi stationary field radiated by the reflectors. Therefore the receiver recognises a variation of the actual power of the reflector (see also **Figure 12**). Interesting enough this fading process does not even come to a stop when the car does not move. We assume that the channel is changing for example due to trees in the wind and other cars. Furthermore there was no correlation between this fading process and the receiver speed. Therefore we assume this process to be time dependent only. The typical bandwidth of such a process is in the range of some Hertz. The deepness of the fades is expressed by the Rice factor K_{Rice}.

$$K_{Rice} = \frac{P_{const}}{P_{fad}} \tag{2}$$

It defines the ratio between the constant power P_{const} and the power of the fading process P_{fad}. **Figure 11** shows the distribution of the Rice factor.

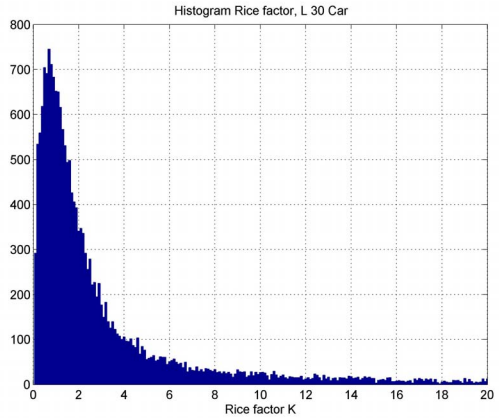

Figure 11: Rice factor histogram of the fading process.

3.6 Time series characteristic of reflectors

Classical channel models like the GSM channel model [7] use time invariant path delays and model the change of the reflector over the time by the assumption that many echoes are received at almost the same path delay and their absolute azimuth is equally distributed. The resulting Doppler spectrum, the so called Jakes spectrum [8], is given by:

$$S(f_D) = \begin{cases} \dfrac{const}{\sqrt{1-\left(\dfrac{f_D}{f_{D\max}}\right)^2}} & \forall \ |f_D| < f_{D\max} \\ 0 & else \end{cases} \tag{3}$$

This approach is feasible for narrow band systems like GSM but in a wide band system such as GPS/GALILEO we regard the modelling accuracy as insufficient. **Figure 12** shows the sliding window

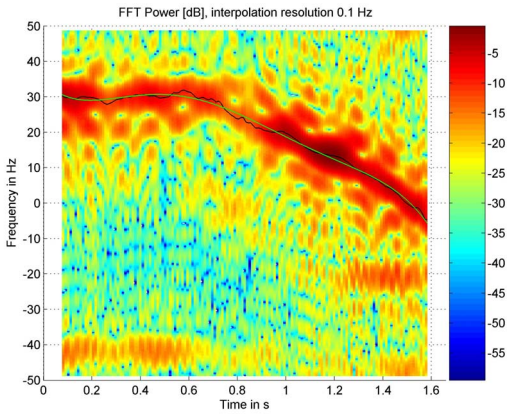

Figure 12: Sliding window Fourier transform of an isolated reflection.

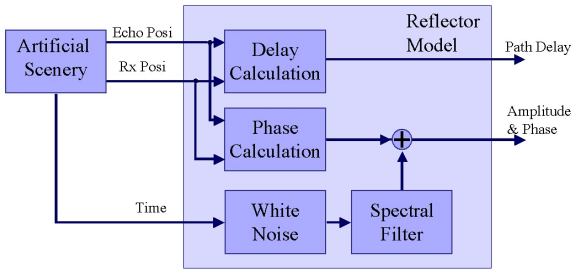

Figure 13: Model of an isolated reflector

Fourier transform of an isolated reflection. There it can be seen that the echo is best characterised by a trace in Doppler frequency. Within 1.6 s the Doppler frequency of the reflector changes from +30 Hz to -5 Hz. In the same period the path delay of the reflector changes. The variability of the reflector is clearly dependent on the vehicle speed. Therefore we implemented the channel model using a geometrical reflector representation. This means we initialise a reflector at a randomly chosen position (according to the measured statistics) and pass by with a receiver with the actual speed. Then both, path delay and phase of the reflection can be calculated geometrically. This causes the main process to be motion dependent only. **Figure 13** shows how a single reflector is modelled. In terms of the reflector the artificial scenery generates a continues series of receiver positions according to the actual speed. The receiver is moving only in x-direction. To simulate turns the relative azimuth of the satellite is changed.

3.7 Number of echoes

During a drive through a city the number of echoes being received changes. For a navigation receiver that tries to estimate the channel impulse response (super resolution for multipath mitigation) a high number of reflections is a ”high stress scenario”. Other phases with a lower number of echoes are less critical. Besides the mean number of echoes it is therefore very important to exactly model this increasing and decreasing process. A sample of it is shown in **Figure 14**. Please note the relatively high number of echoes (up to 50) at the same time. We had been able to detect two processes:

An extremely narrow band process with high power and a lower powered wide band process. Their combination results in a very good approximation of the process.

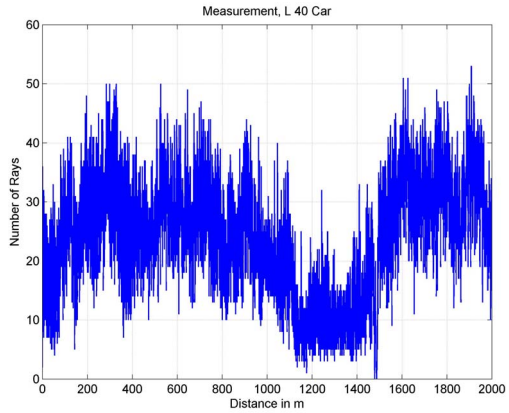

Figure 14: Number of echoes at the same time during a 15 min drive trough a city.

4. CHANNEL MODEL

The block diagram in **Figure 15** gives an overview of the implemented model. The x-coordinate and the relative satellite azimuth are derived from the user speed, user heading and satellite azimuth as explained in section 4.6. This drives the artificial scenery (**Figure 16**) where house fronts, trees and lampposts affect the direct path. Controlled by a number of echo

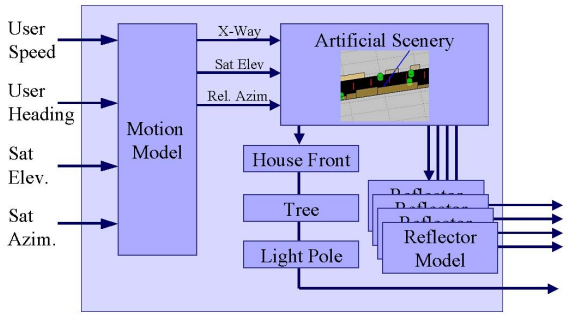

Figure 15: Block diagram of the channel model.

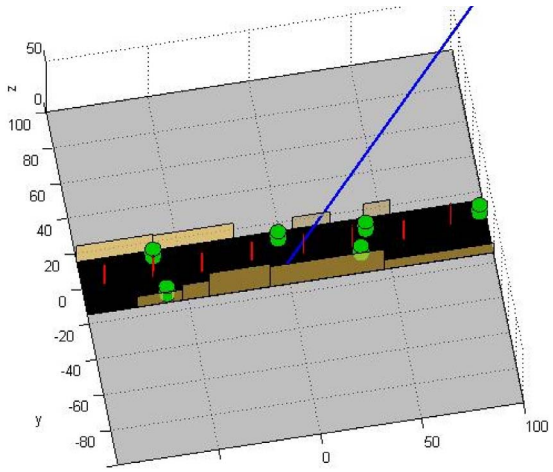

Figure 16: A picture of the artificial scenery. Brown are house fronts, green cylinders are trees, red are poles.

generator the actual amount of reflections is created in the scenery at positions according to the likelihood distribution. The reflectors power, bandwidth, rice factor and lifespan are taken from the statistics. Their delay and phase is therefore changing according to this statistical parameters and according to the receiver movement relative to the reflector position. In **Figure 17** - **Figure 20** an example output of the channel model is given. In this scenario the car drove with a variable speed (using a sin(t) like stop and go function) through the city. At 4.7 s the speed of the vehicle was nearly 0 km/h. In **Figure 18** the Doppler shift of every echo is shown. The red dotted line is the theoretical limit for the Doppler shift given by

$$f_{Doppler} = \frac{\vec{v} \cdot \left(\overrightarrow{RX} - \vec{S} \right)}{c_0} f_C \tag{4}$$

where v is the speed vector of the vehicle, RX is the receiver position, f_C is the carrier frequency, S is the satellite Position and c_0 is the speed of light. In this figure and in the detail (**Figure 20**) one can determine isolated echoes changing their Doppler shift during their life distance (for example the mint green colored echo lasting from 0.81 - 1.35 s). The rapid changes in the channel are visible within the displayed period of around one second many echoes die and others are generated. Around the standstill the channel does not change much - clearly visible by the low Doppler bandwidth and the long lasting echoes (long lines) in **Figure 17**. In this situation only the time driven fading process is changing the channel. But neither an echo is terminated nor a new one is generated in this situation. Furthermore one can see regions where more echoes are present than in others. Due to this precise modelling of reflections new receiver algorithms for e.g. multipath mitigation can be tested in very realistic simulations now. An important improvement

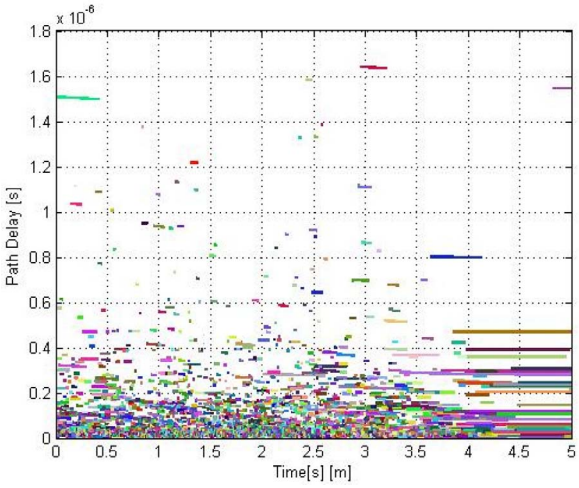

Figure 17: Example of generated echoes. Plotted is the path delay of the reflections over time.

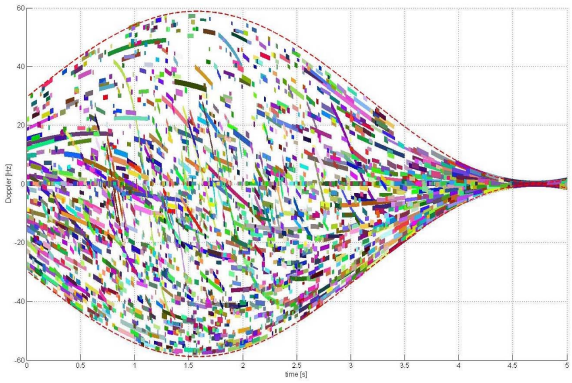

Figure 18: Example of generated echoes. Plotted is the Doppler of the reflections over time

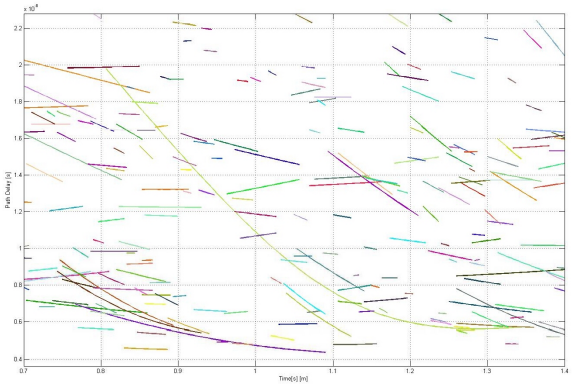

Figure 19: Detail of **Figure 17**.

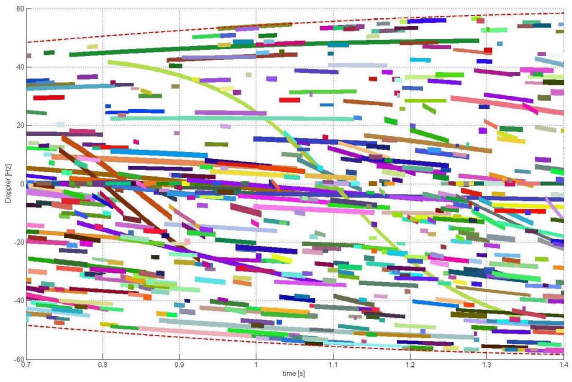

Figure 20: Detail of **Figure 18**.

compared to regular statistical models is the geometrical reflector representation which guarantees the realistic delay and phase correlation among the occurring echoes.

5. SIMULATION

Due to the increasing demand for rail applications we selected this scenario for simulations. To simulate the pseudo range error of a moving receiver we defined a street profile according to a situation at the Lüneburger Straße in Berlin (Germany) which can be surveyed with e.g. Google Earth at coordinates 52°31'18.55" N and 13°21'41.47" E. In this situation we assume a train moving upwards on the right track (-20.75m) as illustrated in **Figure 21**. We defined house fronts at x=-29m and 7.5m. Tree rows are defined at 5 and -4.5m; two rows of poles are at –7m and -24m.

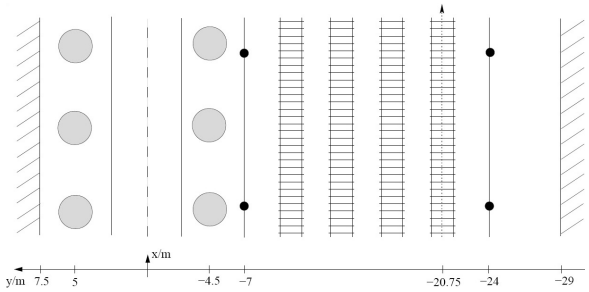

Figure 21: Urban railway environment.

To best possible derive the dependency on the satellite azimuth we selected a rail track that is mostly in a straight line but has still some curves to stress the tracking loops (see **Figure 22**). Again to stress the tracking loops we applied some speed changes to the vehicle, typical for an urban rail run. **Figure 23** shows the speed versus time and clearly indicates four acceleration and five deceleration phases.

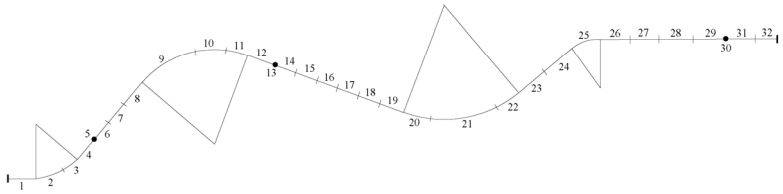

Figure 22: Rail track profile.

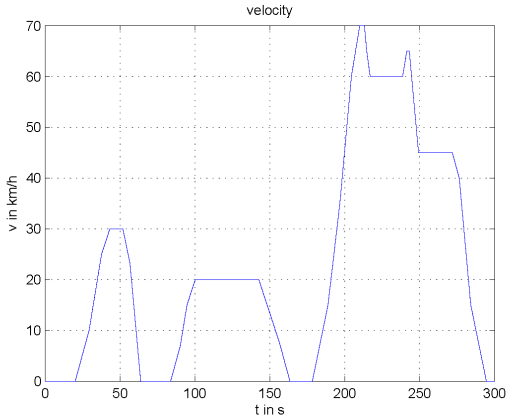

Figure 23: Velocity profile.

For the analysis DLR's signal level simulator NavSim was used in conjunction with the LMS channel model. A standard receiver with a Δ-correlator spacing of 1 chip is simulated, investigating the performance of the GPS C/A signal. **Figure 24** shows the pseudo range error of 20 independent runs for a satellite azimuth of 20 degrees and an elevation of 10 degrees. In this plot the pink areas indicate a situation where the LOS had been blocked by the right house front. White areas indicate clear LOS. The red line is the ideal pseudo range for the specific situation. Not surprising the errors are low in the regions where LOS was present and higher where LOS was shadowed. But even if LOS has been present in a stop phase (e.g. between 60 and 80s) an increased error can be seen. This effect is caused by a slowly varying, strong echo being present over the whole stop period. This effect is of course larger in stop periods with blocked LOS. It can also be seen that a receiver stays in lock even in phases where the LOS is blocked. In these phases it gains most of its power from the reflections.

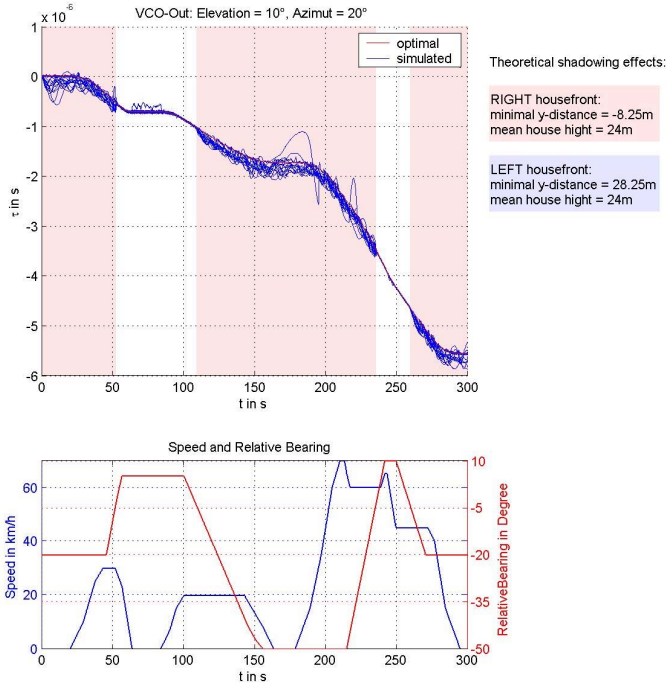

Figure 24: Simulation example 10° elevation and 20° azimuth.

To get an overview on azimuth and elevation dependency we repeated the 20 simulation runs in an azimuth grid of 20 degree steps and an elevation grid of 10 degrees. The result of this is shown in **Figure 25** for the bias and in **Figure 26** for the standard deviation of the pseudo range error. It can clearly be seen that for low elevations (outer circle) the error is significantly higher than for high elevations (inner circle). Furthermore shadowing on the right side (around 90 degrees) by the near right house front causes a significantly higher error than on the left side (around 270 degrees) by the much farer left house front. The minimal error is for 340 and 200 degrees azimuth where in average the satellite was visible at most.

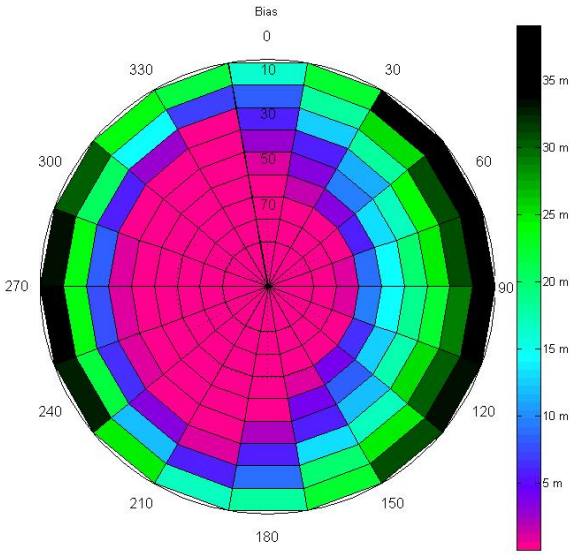

Figure 25: Pseudo range error - bias

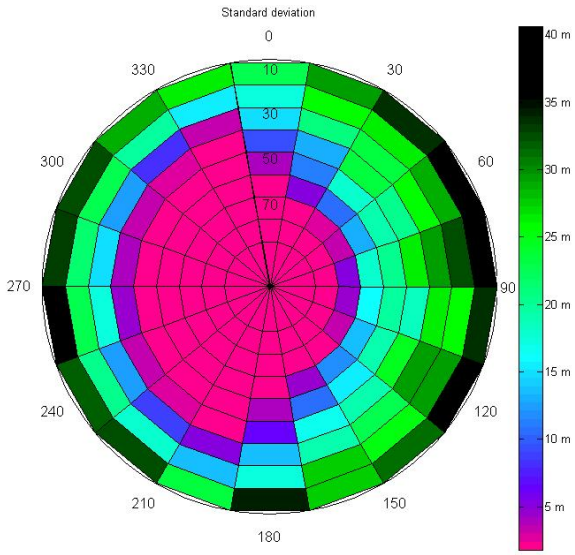

Figure 26: Pseudo range error – standard deviation

6. SUMMARY

We have demonstrated that the new land mobile multipath channel model can be parameterized to be applicable to the urban rail environment. Simulations of this critical scenario show clearly the performance limits of GNSS receivers, dominated by shadowing effects in the urban environment. It is important to note that a clear pseudo range error bias is present in the urban case. Both, the bias and the standard deviation in dependency of the satellites position have been determined and events causing large position errors have been identified. For the future it is planned to investigate the performance of the Galileo signals and of multipath mitigation techniques in this demanding environment.

The presented channel model is based on a new approach: The combination of statistical data from a measurement and a deterministic scenario. The deterministic scenario is used for the direct path modelling. This includes effects such as shadowing by house fronts, tree damping or refracting lampposts. The reflections of this channel model are generated statistically in the geometric scenario. Their generation is driven by data obtained from the measurement only. The model includes:

- Elevation changes,
- azimuth changes,
- speed changes
- and a variable number of reflectors.

Simulations of the critical scenario for rail application show clearly the performance limits of a standard GPS receiver. The dominant error is caused by shadowing in the urban environment. In this situation the receiver can only track echo signals, which is consequently causing large errors. It is also important to note that a pseudo range error bias is present in this application. Both, the bias and the standard deviation have been determined in dependency of the satellites position.

For the future it is planned to investigate the performance of the Galileo signals and of multipath mitigation techniques in this demanding environments.

The channel model is available for download:
http://www.kn-s.dlr.de/satnav/

ACKNOWLEGDEMENT

The presented simulations investigating the urban rail environment were performed in the framework of the GJU project Girasole.

REFERENCES

1. Schweikert R., Wörz T.: "Signal design and transmission performance study for GNSS-2", Tech. note on digital channel model for data transmission, ESA, 1998.
2. Orfanidis J. S.: "Electromagnetic Waves and Antennas", Internet http://www.ece.rutgers.edu/~orfanidi/ewa/, Rutgers University, June 2004.
3. Yvo L. C. de Jong and Matti H. A. J. Herben: "A tree-scattering model for improved propagation prediction in urban microcells", IEEE Transactions on Vehicular Technology, pages 503–513, March 2004.
4. Steingass A., Lehner A.: "Measuring the navigation multipath channel a statistical analysis", ION GPS 2004 Conference Long Beach, California USA, September 2004.
5. Steingass A., Lehner A.: "Measuring Galileo's multipath channel", Global Navigation Satellite Systems Conference (GNSS2003), Graz, Austria, 2003.
6. Esbri-Rodriguez O., Konovaltsev A. and Hornbostel A.: "Modeling of the GNSS directional radio channel in urban areas based on synthetic environments", Proceedings of ION NTM, Jan. 2004.
7. COST 207 WG1: "Proposal on channel transfer functions to be used in GSM tests 1986", Technical report, CEPT Paris, 1986.
8. Jakes W. C.: "Microwave Mobile Communications", John Wiley & Sons, Inc., New York, 1974.